

# Experimental Investigation of the Competing Orders and Quantum Criticality in Hole- and Electron-Doped Cuprate Superconductors

N.-C. Yeh<sup>1</sup>, C.-T. Chen<sup>1</sup>, V. S. Zapf<sup>1</sup>, A. D. Beyer<sup>1</sup>, C. R. Hughes<sup>1</sup>,  
M.-S. PARK<sup>2</sup>, K.-H. KIM<sup>2</sup>, and S.-I. LEE<sup>2</sup>

<sup>1</sup>*Department of Physics, California Institute of Technology, Pasadena, CA 91125, USA*

<sup>2</sup>*Pohang University of Science and Technology, Pohang 790-784, Republic of Korea*

August 4, 2004

We investigate the issues of competing orders and quantum criticality in cuprate superconductors via experimental studies of the high-field thermodynamic phase diagrams and the quasiparticle tunneling spectroscopy. Our results suggest substantial field-induced quantum fluctuations in all cuprates investigated, and their correlation with quasiparticle spectra implies that both electron- (n-type) and hole-doped (p-type) cuprate superconductors are in close proximity to a quantum critical point that separates a pure superconducting (SC) phase from a phase consisting of coexisting SC and a competing order. We further suggests that the relevant competing order is likely a spin-density wave (SDW) or a charge density wave (CDW), which can couple to an in-plane Cu-O bond stretching longitudinal optical (LO) phonon mode in the p-type cuprates but not in the n-type cuprates. This cooperative interaction may account for the pseudogap phenomenon above  $T_c$  only in the p-type cuprate superconductors.

PACS. 74.72.-h - Cuprate superconductors.

PACS. 74.50.+r - Tunneling phenomena.

PACS. 74.25.Dw - Superconductivity phase diagrams.

## I. Introduction

The pairing mechanism of high-temperature superconducting cuprates remains elusive to date, largely because of the existence of competing orders in the ground state of these strongly correlated electronic systems [1, 2, 3], which gives rise to lack of universality in a variety of fundamental physical properties [4, 5, 6]. Amongst different scenarios for cuprate superconductivity, spin- and phonon-mediated pairing mechanisms have been most discussed [4, 7]. The former is considered feasible because of the proximity of all cuprate superconductors to a Mott antiferromagnetic (AFM) insulating state. The latter scenario receives attention because of the correlation between significant softening of a longitudinal optical (LO) in-plane Cu-O stretching phonon mode and the occurrence of superconductivity in some of the p-type cuprates [8]. Given that cuprate superconductors are strongly correlated electronic systems, the spin, charge and lattice degrees of freedom are likely all intertwined, and can cooperate at times to yield enhanced collective phenomena.

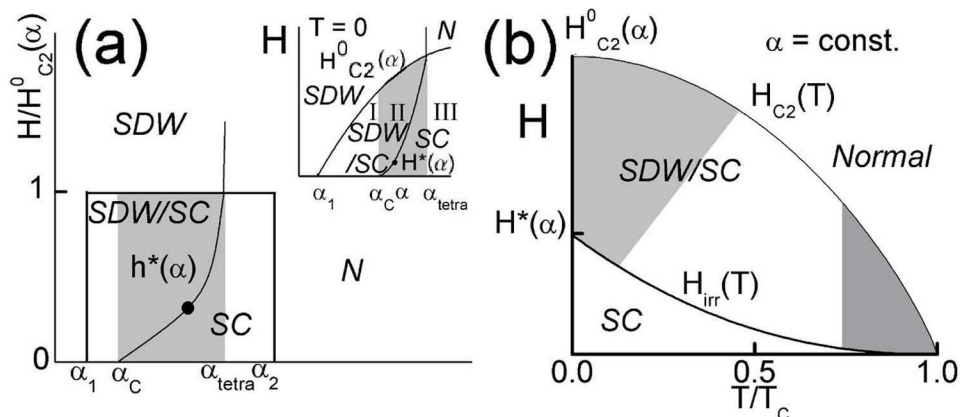


FIG. 1. Schematic phase diagrams of cuprate superconductors with competing SDW and SC: (a) Reduced field  $h = (H/H_{c2}^0)$  vs. material parameter ( $\alpha$ ) phase diagram at  $T = 0$  (main panel), transformed from the phase diagram in the inset[10]. Here  $h^*(\alpha) \equiv H^*(\alpha)/H_{c2}^0$  denotes the phase boundary that separates a pure SC from a coexisting SDW/SC phase, and  $N$  denotes the normal state. (b)  $H(\alpha)$  vs.  $(T/T_c)$  phase diagram for a given  $\alpha$  value. The shaded regime between  $H_{irr}(T \rightarrow 0)$  and  $H_{c2}(T \rightarrow 0)$  is associated with strong quantum fluctuations, and that between  $H_{irr}(T \rightarrow T_c)$  and  $H_{c2}(T \rightarrow T_c)$  is associated with strong thermal fluctuations.

In this work, we attempt to address the issues of competing order and quantum criticality via experimental studies of the high-field thermodynamic phase diagrams and quasiparticle spectroscopy of various p- and n-type cuprates. Our findings of strong field-induced quantum fluctuations in all cuprates and the corresponding correlation with quasiparticle spectroscopy suggest that cuprate superconductors, regardless of being electron- or hole-doped, are all in close proximity to a quantum critical point (QCP) [2, 9] that separates a pure superconducting (SC) state from a coexisting state of SC and a competing order. We shall discuss the relevant competing orders in the context of existing experimental evidence and theory, and also examine the LO phonon-mediated pairing scenario.

## II. Competing orders and quantum criticality

Cuprate superconductors are doped Mott insulators with strong electronic correlation that can result in a variety of competing orders in the ground state [1, 2, 3, 4]. In contrast to conventional superconductivity where the relevant low-energy excitations are dominated by quasiparticles, the presence of competing orders in the cuprates implies that additional channels of low-energy excitations, such as collective modes in the form of SDW [10, 11], CDW [3], or staggered flux (also known as the d-density wave DDW)[12], can either coexist with SC or be induced by increasing magnetic field [10, 11], temperature [13], disorder [2, 14, 15], currents [16, 17], etc. We therefore expect the cuprate superconductors to exhibit significant quantum fluctuations and reduced SC stiffness because of the existence of multiple channels of low-energy excitations.

Indeed, macroscopically all cuprate superconductors are known to be extreme type-II superconductors [18], a reflection of the weak SC stiffness associated with these doped Mott insulators. In addition, the presence of competing orders are likely responsible for the lack of universality in the pairing symmetry, pseudogap, quasiparticle spectral homogeneity, and commensuration of the low-energy spin excitations [4, 5, 6]. The proximity of cuprate SC to competing orders also result in quantum criticality [1, 2, 3, 4, 9]. Hence, it is instructive to investigate the degree of quantum fluctuations and the corresponding quasiparticle spectroscopy of cuprate superconductors in order to unravel the dominant competing order in the ground state.

As a heuristic example, we consider a scenario that cuprate superconductivity occurs near a non-universal QCP at  $\alpha = \alpha_c$  that separates the pure SC phase from a phase with coexisting SC and SDW [10, 11], where  $\alpha$  is a material-dependent parameter that may represent the doping level [2, 9], the electronic anisotropy, spin correlation, orbital ordering, the on-site Coulomb repulsion [13], or the degree of disorder for a given family of cuprates [2, 9], as illustrated in the inset of Fig. 1(a). The scenario of SDW as the relevant competing order can be rationalized by the proximity of cuprate SC to the Mott AFM, and also by experimental evidence for spin fluctuations in the SC state of cuprates [19, 20, 21, 22]. We stress here, however, that our experimental investigation and analysis given below can be generalized to other competing orders without restricting to the SDW.

The  $T = 0$  phase diagram in Fig. 1(a) shows that in the absence of magnetic field  $H$ , the ground state consists of a pure SDW phase if  $\alpha < \alpha_1$ , a SDW/SC coexisting state if  $\alpha_1 < \alpha < \alpha_c$  (Regime I), and a pure SC phase if  $\alpha_c < \alpha \leq \alpha_{tetra}$  (Regime II) or  $\alpha_{tetra} < \alpha < \alpha_2$  (Regime III), where  $\alpha_{tetra}$  denotes a tetra-critical point. Upon applying magnetic field, spin fluctuations can be induced due to magnetic scattering from the  $S = 1$  excitons centered around the vortex cores [10], which can be delocalized with increasing field and lead to a stabilized SDW coexisting with SC for  $H^*(\alpha) < H < H_{c2}^0(\alpha)$  in Regime II, where  $H_{c2}^0(\alpha)$  denotes the upper critical field of a given sample at  $T = 0$ . To quantify the degree of field-induced quantum fluctuations, we consider the normalized quantity  $h^*(\alpha) \equiv [H^*(\alpha)/H_{c2}^0(\alpha)]$ , which transforms the phase diagram in the inset of Fig. 1(a) to that in the main panel. Here the characteristic field  $H^*(\alpha)$  for a given sample can be determined from thermodynamic measurements of the irreversibility line  $H_{irr}(T, \alpha)$  at  $T \rightarrow 0$ , as illustrated in Fig. 1(b). The transformed phase diagram in Fig. 1(a) indicates that a smaller magnitude of  $h^*(\alpha)$  corresponds to a closer proximity to  $\alpha_c$  for a cuprate in Regime II. On the other hand, for a cuprate in Regime I, SDW coexists with SC even in the absence of external fields, implying gapless SDW excitations (i.e.  $\Delta_{SDW} = 0$ ) and strong excess fluctuations in the SC state. Thus, the magnitude of  $h^*(\alpha)$  for a given cuprate correlates with its SC stiffness and anti-correlates with its susceptibility to low-energy excitations. Such correlations can be independently verified via studies of the quasiparticle spectra taken with a low-temperature scanning tunneling microscope (STM).

### III. Experimental Approach and Results

To investigate the conjecture outlined above, we employ in this work measurements of the penetration depth  $\lambda(T, H)$ , magnetization  $M(T, H)$ , and third-harmonic susceptibility  $\chi_3(T, H)$  on different cuprates to determine the irreversibility field  $H_{irr}(T)$  and the upper critical field

$H_{c2}(T)$ . The degree of quantum fluctuations in each sample is estimated by the ratio  $h^* \equiv (H^*/H_{c2}^0)$ , where  $H^*$  is defined as  $H^* \equiv H_{irr}(T \rightarrow 0)$ . The  $h^*$  values thus determined for different cuprates are compared with the corresponding quasiparticle spectra taken with a low-temperature scanning tunneling microscope (STM).

The cuprates studied in this work include the n-type optimally doped infinite-layer cuprate  $\text{La}_{0.1}\text{Sr}_{0.9}\text{CuO}_2$  (La-112,  $T_c = 43$  K) [6] and one-layer  $\text{Nd}_{1.85}\text{Ce}_{0.15}\text{CuO}_{4-\delta}$  (NCCO,  $T_c = 21$  K) [23]; the p-type optimally doped  $\text{HgBa}_2\text{Ca}_3\text{Cu}_4\text{O}_x$  (Hg-1234,  $T_c = 125$  K) and  $\text{YBa}_2\text{Cu}_3\text{O}_{7-\delta}$  (Y-123,  $T_c = 93$  K) [5, 24]. These results are compared with data obtained by other groups on p-type underdoped Y-123 ( $T_c = 87$  K) [25], over- and optimally doped  $\text{Bi}_2\text{Sr}_2\text{CaCu}_2\text{O}_{8+x}$  (Bi-2212,  $T_c = 60$  K and 93 K) [26, 27]; and n-type optimally doped  $\text{Pr}_{1.85}\text{Ce}_{0.15}\text{CuO}_{4-\delta}$  (PCCO,  $T_c = 21$  K) [28]. Details of the synthesis and characterization of various samples have been given elsewhere for Y-123 [5, 24], NCCO [23], La-112 [29], and Hg-1234 [30, 31].

### III-1. Thermodynamic measurements of the high-field phase diagram

To determine  $H_{c2}(T)$ , the penetration depths  $\lambda(T, H)$  of La-112 and Hg-1234 were measured in the pulsed-field facilities up to 65 Tesla at the National High Magnetic Field Laboratory (NHMFL) in Los Alamos by detecting the frequency shift  $\Delta f$  of a tunnel diode oscillator (TDO) resonant tank circuit, with the sample contained in one of the component inductors [32]. Small changes in the resonant frequency can be related to changes in the penetration depth  $\Delta\lambda$  by  $\Delta\lambda \propto -\frac{\Delta f}{f_0}$  [32]. In our case, the reference frequency is  $f_0 \sim 60$  MHz and  $\Delta f \sim (0.16 \text{ MHz}/\mu\text{m})\Delta\lambda$ , as detailed in Ref. [32]. For polycrystalline samples at a constant temperature  $T$ , the onset of deviation of the resonant frequency from that of the normal state signals the maximum upper critical field  $H_{c2}^{ab}(T)$ , as exemplified by La-112. On the other hand,  $H_{c2}^c(T)$  of a polycrystalline sample can be determined by placing a grain-aligned sample in the TDO resonant tank circuit, as exemplified in the inset of Fig. 2(a) for La-112. The  $M(T, H)$  measurements were conducted in high magnetic fields (up to 50 Tesla in a  $^3\text{He}$  refrigerator) using a compensated coil in the pulsed-field facilities, and in lower DC fields using a Quantum Design SQUID magnetometer at Caltech. The irreversibility field  $H_{irr}(T)$  was identified from the onset of reversibility in the  $M(T, H)$  loops, as exemplified in the inset of Fig. 2(b) for  $M$ -vs.- $H$  data of La-112 and in the main panel for  $M$ -vs.- $T$  data of Hg-1234. The third-harmonic magnetic susceptibility  $\chi_3(T, H)$  measurements were also performed on Hg-1234 sample using a 9-Tesla DC magnet and Hall probe techniques [33]. The  $\chi_3(T, H)$  data measured the non-linear response of the sample and were therefore sensitive to the occurrence of phase transformation [33]. These measurements were carried out to independently verify the results from  $M(T, H)$ -vs.- $T$ .

A collection of measured  $H_{irr}^{ab}(T, \alpha)$  and  $H_{c2}^{ab}(T, \alpha)$  curves normalized to the corresponding in-plane  $H_{c2}^0(\alpha) \sim H_p \equiv \Delta_{SC}^0/(\sqrt{2}\mu_B)$  for various cuprates are summarized in the main panel and the inset of Fig. 3(a), respectively. Here  $H_p$  is the paramagnetic field, and  $\Delta_{SC}^0$  denotes the superconducting gap at  $T = 0$ , which can be determined either directly from tunneling data or from the relation  $\Delta_{SC}^0 \sim 2.8k_B T_c$  for under- and optimally doped p-type cuprates. The characteristic fields ( $h^*$ ) of several cuprates are given in Fig. 3(b) for comparison. We note that the Hg-1234 sample, while having the highest  $T_c$  and upper critical field (estimated at  $H_p \sim H_{c2}^{ab} \sim 500$  Tesla) among the cuprates shown here, has the lowest reduced irreversibility line ( $H_{irr}^{ab}(T)/H_p$ ). This phenomenon is not only due to the extreme two-dimensionality (2D)

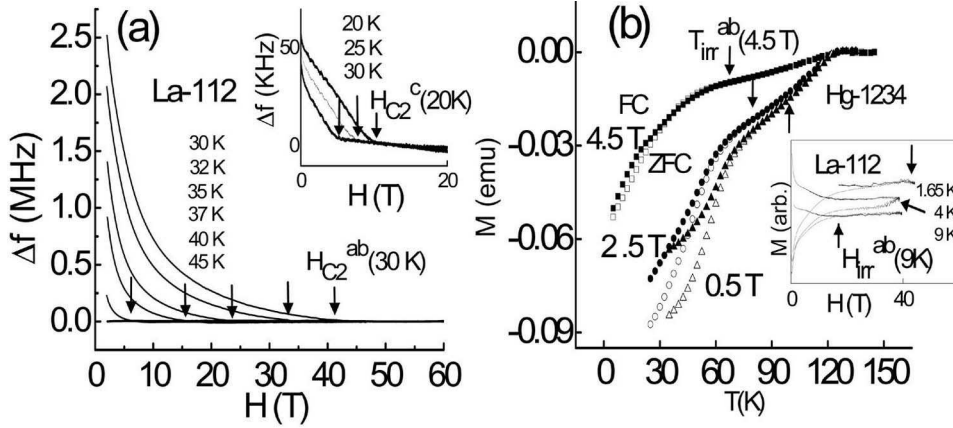


FIG. 2. (a) Selected data for changes in the resonant frequency  $\Delta f$  of the TDO tank circuit relative to the normal state of a polycrystalline La-112 as a function of  $H$  at various  $T$ . The estimated  $H_{c2}^{ab}(T)$  for  $H \parallel ab$ -plane are indicated by arrows. Similar measurements on a grain-aligned La-112 are shown in the inset, which yield  $H_{c2}^c(T)$ . (b) Main panel: representative zero-field-cooled (ZFC) and field-cooled (FC)  $M(T, H)$ -vs.- $T$  data of Hg-1234 taken at  $H = 0.5, 2.5$  and  $4.5$  Tesla, with the corresponding  $T_{irr}^{ab}(H)$  indicated by arrows, using the criterion  $|M_{ZFC}(T_{irr}, H) - M_{FC}(T_{irr}, H)|/|M(T \rightarrow 0, H \rightarrow 0)| \sim 1.5\%$ . The  $T_{irr}^{ab}(H)$  values thus obtained are independently verified from measurements of  $|\chi_3(T, H)|$  (not shown, see Ref. [17] for representative data). Inset:  $M(T, H)$ -vs.- $H$  data on La-112 for  $T = 1.65, 4.0$  and  $9.0$  K, where  $H_{irr}^{ab}(T)$  are indicated by arrows [32].

of Hg-1234 [31] that leads to strong thermal fluctuations at high temperatures, but is also likely the result of its much closer proximity to the QCP, yielding strong field-induced quantum fluctuations at low temperatures. In the context of a  $t$ - $t'$ - $U$ - $V$  model [13], we may consider the varying proximity of optimally doped cuprates Hg-1234, La-112, NCCO and Y-123 to the QCP as a manifestation of the varying on-site Coulomb repulsion  $U$  and pair attraction  $V$  of carriers in the  $\text{CuO}_2$  plane; larger  $U$  (smaller  $V$ ) corresponds to closer proximity to a Mott AFM insulator. Thus, the quantity  $(U/V)$  anti-correlates with  $\alpha$ . We also compare the field-induced anisotropy in the irreversibility fields ( $H_{irr}^{ab}/H_{irr}^c$ ) among different cuprates, and find that all cuprates except Hg-1234 exhibit increasing anisotropy as  $T \rightarrow T_c^-$ , as shown in the inset of Fig. 3(b). The implication of this anomalous temperature dependence requires further investigation.

### III-2. Quasiparticle spectroscopy

To further verify the conjecture that cuprates with smaller  $h^*$  are in closer proximity to a QCP at  $\alpha_c$  and are therefore associated with a smaller SDW gap  $\Delta_{SDW}$  and stronger quantum fluctuations, we examine the SC energy gap  $\Delta_{SC}(T)$  and the quasiparticle low-energy excitations of different cuprates. In Fig. 4(a), we compare the  $\Delta_{SC}(T)$  data of La-112, taken with a low-temperature STM, with those of Bi-2212 and PCCO obtained from intrinsic tunnel junctions [27] and grain-boundary junctions [28], respectively. We find that the rate of decrease

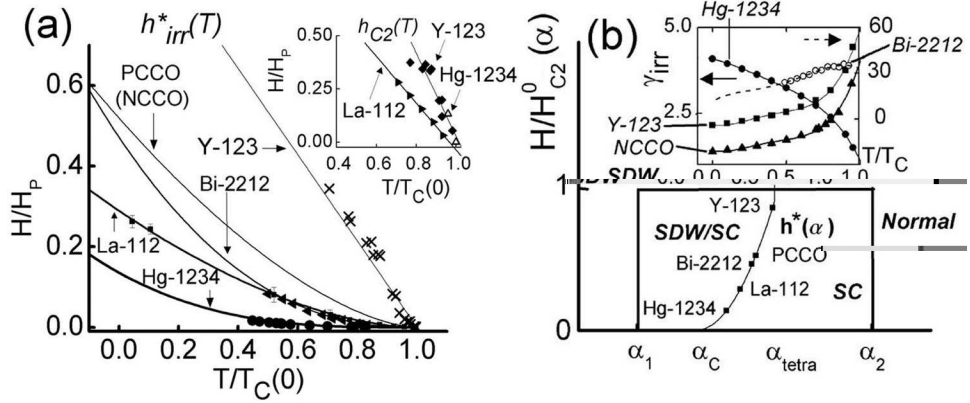


FIG. 3. (a) Comparison of the  $h^*_{irr}(T)$  (main panel) and  $h_{c2}(T)$  (inset) vs.  $(T/T_c)$  phase diagram for Hg-1234, La-112 [32], Bi-2212 [26], NCCO [23, 28], and Y-123 [24, 25] with  $H \parallel$  ab-plane, so that the corresponding  $H_{C2}^0$  is limited by the paramagnetic field  $H_p$ . (b) Main panel: summary of the proximity of different cuprates to a QCP at  $\alpha_c$ . The points along  $h^*$  represent the reduced irreversibility fields obtained from data taken on Y-123, PCCO (NCCO), Bi-2212, La-112, and Hg-1234. Inset: Temperature evolution of the anisotropy of the irreversibility fields ( $\gamma_{irr} \equiv H_{irr}^{ab}/H_{irr}^c$ ). The left (right) scale is for solid (open) symbols.

in  $\Delta_{SC}$  with  $T$  follows the same trend as the decreasing  $h^*$  values for PCCO ( $\sim 0.53$ ), Bi-2212 ( $\sim 0.45$ ), and La-112 ( $\sim 0.24$ ). These differences in  $\Delta_{SC}(T)$  cannot be attributed to different pairing symmetries, because the optimally doped La-112 and NCCO (PCCO) exhibit  $s$ -wave pairing symmetry in the quasiparticle tunneling spectra [6, 34], and Bi-2212 is predominantly  $d_{x^2-y^2}$ -wave pairing [35, 36, 37]. Therefore, the sharp contrast in the  $\Delta_{SC}(T)$  data between La-112 and NCCO (PCCO) suggests that the proximity to the QCP at  $\alpha_c$  plays an important role in determining the low-energy excitations of the cuprates. These experimental findings are consistent with recent  $t$ - $t'$ - $U$ - $V$  model calculations [13] for optimally doped p-type cuprates, which reveal that SDW can be induced thermally even if  $H = 0$ , similar to the field-induced SDW at  $T = 0$ , provided that the material parameter  $\alpha$  falls within Regime II depicted in Fig. 1(a). An example of thermally induced SDW order parameter and the corresponding temperature dependence of the SC order parameter is shown in the inset of Fig. 4(a), following Ref. [13].

Further experimental confirmation for the correlation between  $h^*$  and quantum fluctuations can be realized in the quasiparticle tunneling spectra (the differential conductance  $dI/dV$  vs. biased voltage  $V$ ). As exemplified in Fig. 4(b), we find that excess sub-gap spectral weight relative to the BCS prediction exists in La-112, although the quasiparticle spectra of La-112 are *momentum-independent* and its response to quantum impurities is consistent with  $s$ -wave pairing [6, 38]. The phenomenon cannot be reconciled with simple quasiparticle excitations from a pure SC state, implying the presence of a competing order. In contrast, the quasiparticle spectra on optimally doped Y-123 (for quasiparticle energies  $|E|$  up to  $> \sim \Delta_{SC}$ ) can be explained by the generalized BTK theory [5, 39], as shown in the inset of Fig. 4(b) for averaged quasiparticle tunneling momenta along the  $c$ -axis and along the nodal direction of the  $d_{x^2-y^2}$ -wave pairing

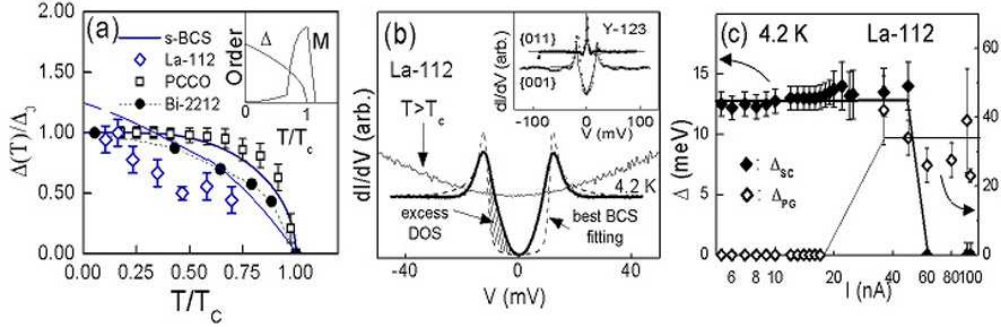


FIG. 4. (a) Comparison of the temperature ( $T$ ) dependence of the normalized SC gap,  $[\Delta_{SC}(T)/\Delta_{SC}^0]$ , for NCCO (PCCO) [28], Bi-2212 [27], and La-112. Inset: temperature evolution of the SC and SDW order parameters ( $\Delta$  and  $M$ ) derived from the  $t$ - $t'$ - $U$ - $V$  model for an optimally doped cuprate with an effective  $\alpha$  in Regime II of Fig. 1(a), after Ref. [13]. (b) Comparison of the normalized quasiparticle spectrum of La-112, obtained using a STM at  $T = 4.2$  K, with the best BCS fitting (dashed line), showing excess sub-gap and reduced post-gap spectral weight. Also shown is the La-112 spectrum taken at  $T > \sim T_c$ , revealing the absence of any quasiparticle pseudogap. Inset: comparison of the normalized quasiparticle tunneling spectra (points) of Y-123 for quasiparticle momenta along c-axis and the nodal direction, taken using a STM at 4.2 K, with the generalized BTK fitting [5, 39] for  $d_{x^2-y^2}$ -wave superconductors (solid line). (c) Evolution of the SC gap  $\Delta_{SC}$  and pseudogap  $\Delta_{PG}$  with the tunneling current  $I$  in La-112 at  $T = 4.2$  K [17].

potential. These results reveal that the spectral contribution from the competing order in Y-123 is insignificant up to  $|E| \sim \Delta_{SC}$ , in agreement with a much larger  $h^*$  value and therefore much weaker quantum fluctuations. Finally, by increasing the tunneling current  $I$ , we observe suppression of the  $\Delta_{SC}$  and emergence of a pseudogap  $\Delta_{PG}$  in the quasiparticle spectra of La-112, as shown in Fig. 4(c), but not in Y-123, again confirming the closer proximity of La-112 to a QCP.

#### IV. Disorder effect, LO phonons, and pseudogap

Next, we consider the effect of disorder on competing orders and SC in the cuprates. Generally speaking, disorder reduces the SC stiffness and shifts  $\alpha$  from Regime II toward Regime I [9]. In this context, a spatially inhomogeneous disorder potential can give rise to spatially varying  $\alpha$  values in a cuprate. In particular, disorder can pin the fluctuating SDW more efficiently in 2D cuprates like Bi-2212 and Hg-1234 than in more 3D cuprates like Y-123 and La-112 [40], so that regions with the disorder-pinned SDW can coexist with SC in the former even if on average  $\alpha > \alpha_c$ . These randomly distributed regions of pinned SDW are scattering sites for quasiparticles at  $T < T_c$  and for normal carriers at  $T > T_c$ . Our recent numerical calculations using the T-matrix approximation [15] have shown that the quasiparticle interference

spectra for SC with coexisting disorder-pinned SDW differ fundamentally from those due to pure SC with random point disorder. In particular, we find that the Fourier transformation (FT) of the quasiparticle local density of states (LDOS) data, obtained from the STM studies of a slightly underdoped Bi-2212 at  $T \ll T_c$  [41, 42], are consistent with the superposition of spectra simulated for SC with random point defects and for SC with randomly pinned SDW regions. In contrast, the FT-LDOS data and the corresponding dispersion relations taken on a similar sample at  $T \gtrsim T_c$  [43] are in good agreement with our simulated results for scattering of holes from disorder-pinned SDW. These findings suggest that a disorder-pinned SDW coexists with SC in Bi-2212 at low temperatures, and that only the SDW persists above  $T_c$  [15].

The aforementioned numerical studies clearly demonstrate the significant role of competing orders in determining the physical properties of cuprate superconductors. In particular, disorder-pinned collective modes such as SDW can account for the strong spatial inhomogeneity observed in the quasiparticle spectra of 2D underdoped cuprates like Bi-2212 below  $T_c$  [44]. Additionally, we suggest that collective modes such as SDW and CDW, which are associated with spin/charge modulations along the Cu-O bonding directions, can couple well with the LO in-plane Cu-O stretching phonon mode in p-type cuprates at moderate temperatures, because the latter is known to involve substantial charge transfer from holes in the oxygen  $2p$ -orbital to the copper  $3d_{z^2}$ -orbital, giving rise to a negative dielectric constant and a local attractive potential [8]. This cooperative effect can result in charge heterogeneity and stabilization of the collective SDW/CDW modes, yielding the pseudogap phenomenon [45] above  $T_c$  in under- and optimally doped p-type cuprates. In contrast, we note that the LO in-plane Cu-O stretching phonon mode cannot incur significant charge transfer in the n-type cuprates as in the p-type, because electron doping in the former primarily resides on the copper site, giving rise to filled  $3d$ - and  $2p$ -orbitals in the  $\text{Cu}^+-\text{O}^{2-}$  bonds, which do not favor phonon-induced charge transfer. We therefore argue that the quantum cooperation effect between the LO phonons and the SDW/CDW collective modes is insignificant in the n-type cuprates, which is consistent with the absence of zero-field pseudogap in the quasiparticle tunneling spectra of n-type cuprates, as exemplified in Fig. 4(b). More importantly, given that the LO phonon-induced attractive potential is not universal in the cuprates, and that similar phonon-induced charge transfer is present in other non-superconducting perovskite oxides [46, 47], the LO phonons are unlikely solely responsible for the superconducting pairing mechanism in the cuprates, even though they might enhance the  $T_c$  values of the p-type cuprate superconductors.

## V. Summary and Remarks

In summary, our experimental studies of the quasiparticle tunneling spectra and the thermodynamic high-field phase diagrams of p- and n-type cuprate superconductors reveal that significant magnetic field-induced quantum fluctuations exist in all cuprate superconductors, and that the degree of quantum fluctuations correlates with the magnitude of excess low-energy excitations as the result of competing orders in the ground state. These experimental results support the notion that the ground state of cuprates is in close proximity to a QCP that separates the SC phase from a coexisting SC and competing order phase, and the competing order is likely associated with a form of collective modes such as the SDW or CDW. Our theoretical anal-

ysis further suggests that the presence of disorder-pinned SDW or CDW in highly 2D cuprates can account for the empirical LDOS both below and above  $T_c$ . Additionally, the presence of SDW or CDW can couple with the LO phonons for the in-plane Cu-O stretching mode in p-type cuprates, because the latter can induce significant transfer of holes from the oxygen  $2p$ -orbital to the copper  $3d_{z^2}$ -orbital, giving rise to a local attractive potential. This quantum cooperation can result in charge heterogeneity and is likely responsible for the pseudogap phenomenon in p-type cuprates. In contrast, the same LO phonons in n-type cuprates do not induce significant charge transfer, which may account for the long-range spectral homogeneity and the absence of zero-field pseudogap in the quasiparticle spectra of n-type cuprates. Hence, the conjecture of LO-phonon mediated pairing mechanism does not seem applicable to all cuprates.

To further our understanding of the competing orders and quantum cooperation of collective modes, systematic studies of the correlation between the low-temperature high-field phase diagrams and the low-energy excitations of more cuprates will be necessary. In particular, neutron scattering studies will be important for determining the SDW gaps and for establishing their relation to quantum fluctuations.

## Acknowledgment

The work at Caltech is supported by the National Science Foundation through Grants #DMR-0405088 and #DMR-0103045, and at the Pohang University by the Ministry of Science and Technology of Korea.

## References

- [1] S.-C. Zhang, *Science* **275**, 1089 (1997).
- [2] S. Sachdev, *Rev. Mod. Phys.* **75**, 913 (2003).
- [3] S. A. Kivelson *et al*, *Rev. Mod. Phys.* **75**, 1201 (2003).
- [4] N.-C. Yeh, *Bulletin of Assoc. Asia Pacific Phys. Soc.* **12**, 2 (2002); cond-mat/0210656.
- [5] N.-C. Yeh *et al*, *Phys. Rev. Lett.* **87**, 087003 (2001).
- [6] C.-T. Chen *et al*, *Phys. Rev. Lett.* **88**, 227002 (2002).
- [7] D. Scalapino, *Phys. Rep.* **250**, 329 (1995).
- [8] M. Tachiki, M. Machida, and T. Egami, *Phys. Rev. B* **67**, 174506 (2003).
- [9] M. Vojta, Y. Zhang and S. Sachdev *Phys. Rev. B* **62**, 6721 (2000).
- [10] E. Demler, S. Sachdev and Y. Zhang, *Phys. Rev. Lett.* **87**, 067202 (2001).
- [11] Y. Chen, H. Y. Chen and C. S. Ting, *Phys. Rev. B* **66**, 104501 (2002).
- [12] J. Kishine, P. A. Lee and X.-G. Wen, *Phys. Rev. Lett.* **86**, 5365 (2001).
- [13] H.-Y. Chen and C. S. Ting, cond-mat/0405524 and cond-mat/0402141 (2004).
- [14] A. Polkovnikov, M. Vojta, and S. Sachdev, *Phys. Rev. B* **65**, 220509 (R) (2002).
- [15] C.-T. Chen and N.-C. Yeh, *Phys. Rev. B* **68**, 220505(R)(2003).

- [16] N.-C. Yeh *et al*, to appear in *Physica C* (2004); cond-mat/0405073.
- [17] N.-C. Yeh *et al*, to appear in *Int. J. Mod. Phys. B* (2004).
- [18] G. Blatter *et al*, *Rev. Mod. Phys.* **66**, 1125 (1994).
- [19] B. O. Wells *et al*, *Science* **277**, 1067 (1997).
- [20] B. Lake *et al*, *Science* **291**, 1759 (2001).
- [21] H. A. Mook *et al*, *Phys. Rev. Lett.* **88**, 097004 (2002).
- [22] K. Yamada *et al*, *Phys. Rev. Lett.* **90**, 137004 (2003).
- [23] N.-C. Yeh *et al*, *Phys. Rev. B* **45**, 5710 (1992).
- [24] N.-C. Yeh *et al*, *Phys. Rev. B* **47**, 6146 (1993).
- [25] J. L. O'Brien *et al*, *Phys. Rev. B* **61**, 1584 (2000).
- [26] L. Krusin-Elbaum *et al*, *Phys. Rev. Lett.* **92**, 097004 (2004).
- [27] V. M. Krasnov *et al*, *Phys. Rev. Lett.* **84**, 5860 (2000).
- [28] S. Kleefisch *et al*, *Phys. Rev. B* **63**, 100507 (2001).
- [29] C. U. Jung *et al*, *Physica C* **366**, 299 (2002).
- [30] M.-S. Kim *et al*, *Phys. Rev. B* **57**, 6121 (1998).
- [31] M.-S. Kim *et al*, *Phys. Rev. B* **63**, 134513 (2001).
- [32] V. S. Zapf *et al*, submitted to *Phys. Rev. B* (2004); cond-mat/0405072.
- [33] D. S. Reed *et al*, *Phys. Rev. B* **51**, 16448 (1995).
- [34] L. Alff *et al*, *Phys. Rev. Lett.* **83**, 2644 (1999).
- [35] Ch. Renner *et al*, *Phys. Rev. Lett.* **80**, 149 (1998).
- [36] S. H. Pan *et al*, *Nature* **403**, 746 (2000).
- [37] E. W. Hudson *et al*, *Nature* **411**, 920 (2001).
- [38] N.-C. Yeh *et al*, *J. Low Temp. Phys.* **131** 435 (2003).
- [39] J. Y. T. Wei *et al*, *Phys. Rev. Lett.* **81**, 2542 (1998).
- [40] N.-C. Yeh and C.-T. Chen, *Int. J. Mod. Phys. B* **17** 3575 (2003).
- [41] J. E. Hoffman *et al*, *Science* **297**, 1148 (2002).
- [42] K. McElroy *et al*, *Nature* **422**, 592 (2003).
- [43] M. Vershinin *et al*, *Science* **303**, 1995 (2004).
- [44] K. M. Lang *et al*, *Nature* **415**, 412 (2002).
- [45] T. Timusk and B. Statt, *Rep. Prog. Phys.* **62**, 61 (1999).
- [46] J. M. Tranquada *et al*, *Phys. Rev. Lett.* **88**, 075505 (2002).
- [47] W. Reichardt and M. Braden, *Physica B* **263-264**, 416 (1998).